A comprehensive model to describe light scattering properties of cometary dust

Ingrid Mann [a,*], Hiroshi Kimura [a], Ludmilla Kolokolova [b]

[a] *Institut für Planetologie, Westfälische Wilhelms-Universität, Wilhelm-Klemm-Straße 10, D-48149 Münster, Germany*

[b] *Department of Astronomy, University of Florida, 211 SSRB, Gainesville, FL 32605, USA*

Abstract

We present a model of cometary dust that could provide the correct behaviour of the main observational characteristics in the visual spectral regime. The model reproduces the right shape in angular dependencies of intensity and polarisation as well as their spectral gradients (colours) including the change of colour with scattering angle. The dust particles are described as aggregates of a large number of constituent spheres of radius equal to ~ 0.1 μm. We use a refractive index that is characterized by high values of its real and imaginary parts both increasing with wavelength. This refractive index reproduces the comet-Halley element content of dust derived from in-situ measurements but the values are typical, in general for carbonaceous materials. The assumed composition is also in a good agreement with laboratory studies of interplanetary dust particles as well as with the current understanding of the material evolution in comets, although further studies of comet dust properties should include a comparison with thermal observations.

Key words: cometary dust, light scattering, T-matrix method, geometric albedo, refractive index, linear polarisation, aggregate particles
PACS: 42.25.Fx, 42.25.Ja, 47.53.+n, 95.75.−z, 95.85.Kr, 96.50.Dj, 96.50.Gn

* Corresponding author. Fax: +49 251 83 36301
Email addresses: imann@uni-muenster.de (Ingrid Mann), kimura@uni-muenster.de (Hiroshi Kimura), ludmilla@astro.ufl.edu (Ludmilla Kolokolova).

1 Introduction

1.1 Observations

Studies of cometary dust brightness and polarisation reveal the average properties of the grains that contribute to the observed scattered light. In spite of the variety of the possible regions of cometary origin, as well as the variety of formation and evolution temperatures, and dynamical evolutions, the optical properties of cometary dust have common basic characteristic features [1]. These lie in the dependencies of the intensity and polarisation of scattered light on phase angle and wavelength. These properties are derived from astronomical observations where the phase angle is identical to the angle Sun-comet-Earth, α. This angle in the single particle scattering problem (note that multiple scattering is negligible) is related to the scattering angle θ as $\alpha = 180^\circ - \theta$.

Some of the average optical properties are similar (but not identical) to those derived from zodiacal light observations for interplanetary dust (cf. [2,3]). The main common features of light scattering by cometary dust are:

(1) The geometric albedo A, which is related to the intensity of scattered light, is low, $A < 0.05$, at small phase angles.
(2) The intensity I has its maximum at large phase angles, i.e. in the forward scattering regime, flattens at medium phase angles and increases moderately at small phase angles in the backscattering regime.
(3) The polarisation P is slightly negative for small phase angles, α, rises to $P = 0$ at the so-called inversion angle, α_0 of the order of 20° and then it rises to a broad maximum peaking near $\alpha = 90$ to 100°.
(4) Both intensity and polarisation increase with wavelength λ, i.e., show red colour $dI/d\lambda > 0$ and $dP/d\lambda > 0$.
(5) The colour of intensity does not show a clear correlation with phase angle at $\alpha < 70^\circ$, but the polarimetric colour $dP/d\lambda$ increases with phase angle at $\alpha > 30^\circ$.

1.2 Comparison to light scattering models

Having a low albedo is typical for cosmic dust. For example, interpretation of the brightness observations of zodiacal light together with the flux rates derived from space measurements became possible only under the assumption that interplanetary dust particles are very dark [2]. For a long time such a low albedo of grains was explained by the fact that they not only contain dark material but also have a very fluff, porous structure [4,5]. This type of grains

also could reproduce the general trends in intensity and polarisation confirmed by laboratory measurements at irregular particles [2,6] and various types of light scattering calculations of rough-surface particles (see, e.g. [7]). Attempts to reproduce the trends in intensity and polarisation using other types of particles could not provide a consistent model of the dust: a low maximum polarisation can be obtained for non-spherical dark particles [8], while negative polarisation at backscattering requires transparent material [9]; the variation of intensity with phase angle can be explained with the scattering of spheroids of moderate sizes (0.5 to 2 μm) [10] but the shape of the polarisation curve and positive polarimetric colour are better explained with mixtures of submicron particles [11].

Models of aggregates of submicron particles reproduce relatively well the observational data for cometary grains (see Table 1), although not all of the listed calculations were aimed toward describing the cometary dust properties. They also agree with common understanding of the formation of cometary dust from aggregation of interstellar grains (see [26]). We conclude that models where the size parameter of monomers is close to unity, i.e. the size of monomers is of the order of 0.1 μm, in general yield acceptable agreement to the observational data, as long as the aggregate particles are not too small. Aggregates where the number of monomers is less than 60 fail to reproduce the light scattering characteristics. Hence, although the particles are described as fluffy aggregates, a mixture of small single particles does not produce the observed scattering properties. Neither do models, where the size parameters of monomers are either very small or very large compared to unity obtain a good fit to the data. Simulation of cometary dust using aggregate models can sufficiently reproduce the angular dependences of brightness and polarisation as well as positive polarimetric colour when the aggregates are assumed to consist of submicron particles. However, these models still have a great difficulty to reproduce the red colour and the increase of polarimetric colour with phase angle observed for cometary dust [27]. Among the models with the suitable monomer size, those with a large refractive index give the best agreement. Recently, our preliminary results have shown that all the general trends in light scattering by cometary dust can be achieved with an aggregate consisting of optically dark submicron grains [23]. We follow up this study in detail with more refined calculations in order to confirm our model.

2 Model assumptions

2.1 Refractive index

We assume that cometary dust consists of three type of compounds: carbonaceous materials, iron-free silicates and metals, and that the compounds are made of six elements: C, N, O, Mg, Si, and Fe [28]. Once the abundances of the elements are known, we can assign C, N and O to carbonaceous materials; Si, Mg and O to iron-free silicates; and Fe to metal. We shall use the average elemental abundances of C, N, O, Mg, Si and Fe measured in situ for dust in comet Halley [29]. Table 2 summarises the abundance of the j-th element in the i-th compound, X_{ij}, derived from the Halley's data. Also given are the atomic weight of the j-th element, A_j and the bulk density of the i-th compound, ρ_i.

We shall estimate the volume fraction of each compound, f_i, as follows: (1) multiply the j-th atomic number to the elemental abundance to obtain the relative mass of the j-th element in the i-th compound, (2) sum up the relative mass for each composition to obtain the mass ratio for the compounds, (3) divide the mass ratio for each compound by its bulk density to obtain the volume ratio for the compounds and (4) normalize the volume ratio to finally obtain the volume fractions of the compounds. These procedures can be written as

$$f_i = \rho_i^{-1} \sum_{j=1}^{6} X_{ij} A_j / \sum_{i=1}^{3} \rho_i^{-1} \sum_{j=1}^{6} X_{ij} A_j. \tag{1}$$

Inserting the values of ρ_i, A_j and X_{ij} from Table 2 into Equation (1), we obtain the volume fraction of carbonaceous material, silicate and metal to be 0.6568, 0.3176 and 0.0256. We further assume that one third of carbonaceous material is in the form of organic refractory and two third in the form of amorphous carbon. This is consistent with the nitrogen depletion in cometary dust compared to interstellar dust, indicating that one third of organics in cometary dust was transformed into amorphous carbon [33].

We apply the Maxwell-Garnett mixing rule to derive the average refractive indices of cometary dust consisting of carbonaceous material, silicate and metal from the Halley's dust composition. Assuming that organic refractory, silicate and metal are inclusions embedded in amorphous carbon, the average dielectric function, $\varepsilon_{\rm av}$, is then calculated by (see [34])

$$\varepsilon_{\rm av} = \varepsilon_{\rm m} \frac{1 - \sum_{i=1}^{3} f_i + 3 \sum_{i=1}^{3} f_i \varepsilon_i (\varepsilon_i + 2\varepsilon_{\rm m})^{-1}}{1 - \sum_{i=1}^{3} f_i + 3\varepsilon_{\rm m} \sum_{i=1}^{3} f_i (\varepsilon_i + 2\varepsilon_{\rm m})^{-1}}, \tag{2}$$

where ε_i and f_i denote the dielectric function and volume fraction of the i-th inclusion, respectively, and $\varepsilon_{\rm m}$ is the dielectric function of the matrix. Table 3 gives the volume fractions and the refractive indices of amorphous carbon, organic refractory, silicate and metal used for the estimate of $\varepsilon_{\rm av}$ from Equation 2 [30–32]. Note that the complex refractive index, m, is related to the dielectric function, ε, as $\varepsilon = m^2$. Inserting the values of $\varepsilon_{\rm m}$, ε_i and f_i from Table 3 into Equation (2), we obtain the average refractive indices, $m_{\rm av} = 1.88 + 0.47{\rm i}$ at a wavelength of $\lambda = 450$ nm and $m_{\rm av} = 1.98 + 0.48{\rm i}$ at $\lambda = 600$ nm.

2.2 Morphology

We model cometary dust as aggregate particles consisting of identical spheres (monomers) and consider two types of aggregations that result in different morphologies. One is ballistic cluster-cluster aggregation (BCCA), in which particles grow by sticking of identical clusters moving in ballistic trajectories. The other is ballistic particle-cluster aggregation (BPCA), in which particles grow by sticking of single monomers moving in ballistic trajectories. We note that these models are not assumed as the formation process of the cometary dust but rather applied to describe the irregular structure. We perform 3-D numerical simulations to model these aggregate particles based on a Monte-Carlo method to randomize the initial condition of the impactors [39]. We assume that the radius of monomers is $a_{\rm m} = 0.1$ μm and consider the number of monomers $N = 64$, 128, and 256. The assumed monomer size is in agreement with laboratory studies of interplanetary dust [40]. Using different seed numbers for the random generator, we construct three BCCA particles and three BPCA particles for each size of aggregate.

3 Light scattering calculations

We present the geometric albedo A and linear polarisation P as a function of phase angle α and wavelength λ. The geometric albedo is given as $A = (S_{11}\lambda^2)/(4\pi G)$, where S_{11} denotes the orientation-averaged $(1,1)$ component of the scattering matrix and G the geometric cross section [5]. We estimate the surface area $4G$ of aggregates using a Monte-Carlo method [39]. The linear polarisation is given as $P = -S_{12}/S_{11}$, where S_{12} denotes the orientation-averaged $(1,2)$ component of the scattering matrix [34]. We calculate the values of S_{11} and S_{12} using the superposition T matrix method [13].

Figure 1 shows A and P calculated for BPCA (symbols) and BCCA (lines)

particles with number of monomers $N = 64$, 128, 256 at $\lambda = 450$ and 600 nm. The values are averaged over three particles, but the results for the single aggregates are found to be almost identical.

One can see that all the characteristics listed in the introduction are qualitatively satisfied: the intensity has forward scattering and slight backscattering peaks and is rather flat at medium angles; the polarisation function has a bell-type shape with the maximum around 90° and a shallow negative polarisation branch at small phase angles; the colour is red and changes very weakly with the phase angle; the polarimetric colour is also red and increases with phase angle within the phase angles of 0° to 90°. We believe that this qualitative fit to all observational facts is a better indication of a successful model than a quantitative fit to some data that contradicts to others. Nevertheless, this result has to be discussed in the light of experimental results and model assumptions.

4 Discussion

The presented model achieves qualitative agreement to all the observed optical characteristics of cometary dust. While for the calculated cases of particle sizes the obtained maximum polarisation is higher than the observed values we expect the maximum polarisation to decrease to larger particle sizes while at the same time the negative polarisation decreases. This trends are expected from other studies [41] and in Figure 1 can be seen for the negative polarisation.

The importance of the assumed scattering properties lies in the assumption of the refractive index, namely, not only in the fact that it is absorbing but also in the increasing slope with λ. Considering its spectral variation, an increase of both n and k is most suitable for obtaining the optical properties. Our approach is tempting since it may account for all observational trends within one particle model and at the same time it accounts for the mineral composition of cometary dust. Nevertheless some restrictions have to be seen. The refractive index of the monomer material was determined by the Maxwell-Garnett mixing rule, describing the material as a matrix with inclusions of other materials. This is applicable if the size of the inclusions is small compared to the wavelength. The application of the Maxwell-Garnett mixing rule also implies the different constituent materials to be evenly distributed within the monomers. The dust measurements at comet Halley indicate the different dust components to be mixed down to the smallest sizes [42] which may give this method of estimating the refractive index some justification. The $^{12}C/^{13}C$ isotope ratios [29] vary from particle to particle. This indicates that there has been no process leading to chemical homogeneity in the history of cometary dust. By applying the Maxwell-Garnett mixing rule for calculating the index

of refraction we emphasize the contribution of carbonaceous material, since it is assumed as the matrix material in which the other materials are embedded. Moreover, this description does not account for possible interactions between the inclusions and we speculate this may cause some incorrectness for the case of a high percentage of inclusions. In spite of the above mentioned limitations of the Maxwell-Garnett mixing rule, we expect that the average refractive index of cometary dust is close to the one we have derived here.

The measurements at comet Halley [29] show that the detected particles differ from each other and namely the amount of the light elements CHON, assumed to account for the organic refractories, versus the heavier rock forming elements is variable. Since the carbonaceous monomers are relatively dark, we can expect them to determine the scattering properties of an aggregate even when other types of monomers exist. This needs to be checked with further model calculations. We also have to check the common assumption that cometary dust is best described as agglomerates of core-mantle particles [43]. For the case of the core-mantle model, we can assume that the scattering properties of the monomers with core-mantle structure are similar to the mantle material, if the mantle occupies sufficiently large volume compared to the core. Aside from the possibility of these core-mantle particles, also the influence of non-sphericity on the scattering properties has to be investigated in future.

The fact that both albedo and polarisation show a smooth slope as function of the phase angle should not be over-emphasized since this may partly stem from observational averaging. Observations obtained before the 1990's have not been made with imaging detectors [44]. The recent, spatially resolved observations, however, show radial gradients and localized structures in the polarisation data [45,46] as well as higher polarisation in the region of coma jets [46–49]. Hence polarisation differences between comets cannot be distinguished from effects of different observation geometries.

Dobrovolsky et al. [50] and subsequently Levasseur- Regourd et al. [51] suggest based on a comparison of the polarimetric properties of cometary dust at large phase angles that those indicate the existence of two classes of comets for which the optical, linear polarisation vs. phase angle relations of comets fall into two distinct groups. Best-distinguished at large phase angles, the high polarisation comets (including West 1976 VI, P/Halley 1986 III and Levy 1990 XX) have maximum polarisations $P_{\max} \approx 30\%$ while the low polarisation comets (e.g. Kobayashi-Berger-Milon 1975 IX, Austin 1990 V) have $P_{\max} \approx 20\%$. The samples of comets that Levasseur-Regourd et al. [51] suggest show no clear relationship to the dynamical properties of the comets. It should be noted that the recent numerous observations of comet Hale-Bopp do not clearly fit within these two groups [44,52,53]. From our model calculations we expect differences in the optical properties of dust to stem predominantly from different sizes of the grains. If this turns out to be the case the distinction of comets into two

groups requires the presence of two distinct size distributions of dust among a variety of comets, which we think is unlikely.

Our current model needs improvement by refined model calculations. Calculations are in progress and we expect obtaining a better, quantitative fit to the observed data as well as to investigate in detail how the observational characteristics change with changing the model parameters. It should further be discussed how it agrees with the models of material evolution. Comparison to thermal emission models is needed in order to allow for a comparison to further observational data.

Acknowledgements

We would like to thank Daniel Mackowski, Kirk Fuller, and Michael Mishchenko for making their TMM code available. This research has been supported by the German Aerospace Center *DLR* under the project "Kosmischer Staub: Der Kreislauf interstellarer und interplanetarer Materie" (RD-RX-50 OO 0101-ZA) and NASA "Planetary atmospheres" program.

References

[1] Kolokolova L, Hanner MS, Levasseur-Regourd A-Ch, Gustafson BÅS. Physical properties of cometary dust from light scattering and emission. In: Festou M, Keller U, Weaver H, editors. Comets II. Tucson: University of Arizona, 2004. in press.

[2] Weiss-Wrana K. Optical properties of interplanetary dust: comparison with light scattering by larger meteoritic and terrestrial grains. Astron Astrophys 1983;126:240–250.

[3] Levasseur-Regourd AC, Dumont R, Renard JB. A comparison between polarimetric properties of cometary dust and interplanetary dust particles. Icarus 1990;86:264–272.

[4] Giese RH, Weiss K, Zerull RH, Ono T. Large fluffy particles: A possible explanation of the optical properties of interplanetary dust. Astron Astrophys 1978;65:265–272.

[5] Hanner MS, Giese RH, Weiss K, Zerull R. On the definition of albedo and application to irregular particles. Astron Astrophys 1981;104:42–46.

[6] Gustafson BÅS, Kolokolova L. A systematic study of light scattering by aggregate particles using the microwave analog technique: Angular and wavelength dependence of intensity and polarization. J Geophys Res 1999;104:31711–31720.

[7] Mukai S, Mukai T, Kikuchi S. Scattering properties of cometary dust based on polarimetric data. In: Levasseur-Regourd AC, Hasegawa H, editors. Origin and Evolution of interplanetary Interplanetary Dust. Dordrecht: Kluwer, 1991. p. 249–252.

[8] Mishchenko MI, Travis LD. Light scattering by polydisperse, rotationally symmetric nonspherical particles: linear polarization. J Quant Spectrosc Radiat Transfer 1994;51:759–778.

[9] Lumme K, Rahola J, Comparison of light scattering by stochastically rough spheres, best-fit spheroids and spheres. J Quant Spectrosc Radiat Transfer 1998;60:439–450.

[10] Mishchenko MI, Travis LD, Kahn RA, West RA, Modeling phase functions for dustlike tropospheric aerosols using a shape mixture of randomly oriented polydisperse spheroids. J Geophys Res 1997;102:16831–16847.

[11] Mishchenko MI. Light scattering by size-shape distributions of randomly oriented axially symmetric particles of a size comparable to a wavelength. Appl Opt 1993;32:4652–4666.

[12] Draine BT, Flatau PJ. Discrete-dipole approximation for scattering calculations. J Opt Soc Am A 1994;11:1491–1499.

[13] Mackowski DW, Mishchenko MI. Calculation of the T matrix and the scattering matrix for ensembles of spheres. J Opt Soc Am A 1996;13:2266–2278.

[14] West RA. Optical properties of aggregate particles whose outer diameter is comparable to the wavelength. Appl Opt 1991;30:5316–5324.

[15] Kozasa T, Blum J, Okamoto H, Mukai T. Optical properties of dust aggregates II. Angular dependence of scattered light. Astron Astrophys 1993;276:278–288.

[16] Lumme K, Rahola J. Light scattering by porous dust particles in the discrete-dipole approximation. Astrophys J 1994;425:653–667.

[17] Lumme K, Rahola J, Hovenier JW. Light scattering by dense clusters of spheres. Icarus 1997;126:455–469.

[18] Xing Z, Hanner MS. Light scattering by aggregate particles. Astron Astrophys 1997;324:805–820.

[19] Levasseur-Regourd AC, Cabane M, Worms JC, Haudebourg V. Physical properties of dust in the solar system: Relevance of a computational approach and of measurements under microgravity conditions. Adv Space Res 1997;20:(8)1585–(8)1594.

[20] Nakamura R, Okamoto H. Optical properties of fluffy aggregates as analogue of interplanetary dust particles. Adv Space Res 1999;23:(7)1209–(7)1212.

[21] Petrova EV, Jockers K, Kiselev NN. Light scattering by aggregates with sizes comparable to the wavelength: An application to cometary dust. Icarus 2000;148:526–536.

[22] Kimura H. Light-scattering properties of fractal aggregates: numerical calculations by a superposition technique and the discrete-dipole approximation. J Quant Spectrosc Radiat Transfer 2001;70:581–594.

[23] Kimura H, Kolokolova L, Mann I. Optical properties of cometary dust: Constraints from numerical studies on light scattering by aggregate particles. Astron Astrophys 2003;407:L5–L8.

[24] Haudebourg V, Cabane M, Levasseur-Regourd A-C. Theoretical polarimetric responses of fractal aggregates, in relation with experimental studies of dust in the solar system. Phys Chem Earth C 1999;24:603–608.

[25] Petrova EV, Jockers K, Kiselev NN. Light scattering by aggregate particles comparable in size to wavelength: Application to cometary dust. Solar System Res 200;35:57–69.

[26] Greenberg JM, Li A. Morphological structure and chemical composition of cometary nuclei and dust. Space Sci Rev 1999;90:149–161.

[27] Kolokolova L, Kimura H, Mann I. Characterization of dust particles using photopolarimetric data: Example of cometary dust. In: Videen G, Yatskiv YS, Mishchenko MI, editors. Photopolarimetry in Remote Sensing. Dordrecht: Kluwer Academic Publisher, 2004. in press.

[28] Jessberger EK. Rocky cometary particulates: their elemental, isotopic and mineralogical ingredients. Space Sci Rev 1999;90:91–97.

[29] Jessberger EK, Christoforidis A, Kissel J. Aspects of the major element composition of Halley's dust. Nature 1988;332:691–695.

[30] Greenberg JM, Hage, JI. From interstellar dust to comets: a unification of observational constraints. Astrophys J 1990;361:260–274.

[31] Draine BT, Lee HM. Optical properties of interstellar graphite and silicate grains. Astrophys J 1984;285:89–108.

[32] Weast RC. CRC Handbook of Chemistry and Physics. Florida: CRC Press, 1985.

[33] Kimura H, Mann I. Material processing of interstellar dust in comets. In: Engvold O, editor. Highlights of Astronomy. San Francisco: Astronomical Society of the Pacific Press, 2004. in press.

[34] Bohren CF, Huffman DR. Absorption and Scattering of Light by Small Particles. New York: Wiley-Interscience, 1983.

[35] Rouleau F, Martin PG. Shape and clustering effects on the optical properties of amorphous carbon. Astrophys J 1991;377:526–540.

[36] Li A, Greenberg JM. A unified model of interstellar dust. Astron Astrophys 1997;323:566–584.

[37] Laor A, Draine BT. Spectroscopic constraints on the properties of dust in active galactic nuclei. Astrophys J 1993;402:441–468.

[38] Johnson PB, Christy RW. Optical constants of transition metals: Ti, V, Cr, Mn, Fe, Co, Ni, and Pb. Phys Rev B 1974;9:5056–5070.

[39] Kitada Y, Nakamura R, Mukai T. Correlation between cross section and surface area of irregularly shaped particle. In: Maeda M, editor. The Third International Congress on Optical Particle Sizing. Yokohama: Keio University, 1993. p. 121–125.

[40] Brownlee DE. Microparticle studies by sampling techniques. In: McDonnell JAM, editor. Cosmic Dust. New York: Wiley-Interscience, 1978. p. 295–336.

[41] Kimura H, Mann I. Light scattering by large clusters of dipoles as an analog for cometary dust aggregates. J Quant Spectrosc Radiat Transfer 2004; accepted for publication in this volume.

[42] Mann I, Jessberger EK. The in-situ study of solid particles in the solar system. In: Henning T editor. Astromineralogy. Berlin: Springer, 2003. p. 198–216.

[43] Greenberg JM, Li A. Tracking the organic refractory component from interstellar dust to comets. Adv Space Res. 1999;24:(4)497–(4)504.

[44] Kiselev NN, Velichko FP. Aperture polarimetry and photometry of comet Hale-Bopp. Earth Moon Planets 1999;78:347–352.

[45] Kolokolova L, Jockers K, Gustafson BÅS, Lichtenberg G. Color and polarization as indicators of comet dust properties and evolution in the near-nucleus coma. J Geophys Res 2001;106:10113–10127.

[46] Jockers K, Rosenbush VK, Bonev T, Credner T. Images of polarization and colour in the inner coma of comet Hale-Bopp. Earth Moon Planets 1997;78:373–379.

[47] Eaton N, Scarrott SM, Warren-Smith RF. Polarization images of the inner regions of Comet Halley. Icarus 1988;76:270–278.

[48] Hasegawa H, Ichikawa T, Abe S, Hamamura S, Ohnishi K, Watanabe J. Near-infrared photometric and polarimetric observations of comet Hale-Bopp. Earth Moon Planets 1997;78:353–358.

[49] Furusho R, Suzuki B, Yamamoto N, Kawakita H, Sasaki T, Shimizu Y, Kurakami T. Imaging polarimetry and color of the inner coma of comet Hale-Bopp(C/1995 O1). Publ Astron Soc Japan 1999;51:367–373.

[50] Dobrovolsky OV, Kiselev NN, Chernova GP. Polarimetry of comets: A review. Earth Moon Planets 1986;34:189–200.

[51] Levasseur-Regourd AC, Hadamcik E, Renard JB. Evidence for two classes of comets from their polarimetric properties at large phase angles. Astron Astrophys 1996;313:327–333.

[52] Manset N, Bastien P. Polarimetric observations of Comets C/1995 O1 Hale-Bopp and C/1996 B2 Hyakutake. Icarus 2000;145:203–219.

[53] Hadamcik E. Levasseur-Regourd AC. Dust evolution of comet C/1995 O1 (Hale-Bopp) by imaging polarimetric observations. Astron Astrophys 2003;403:757–768.

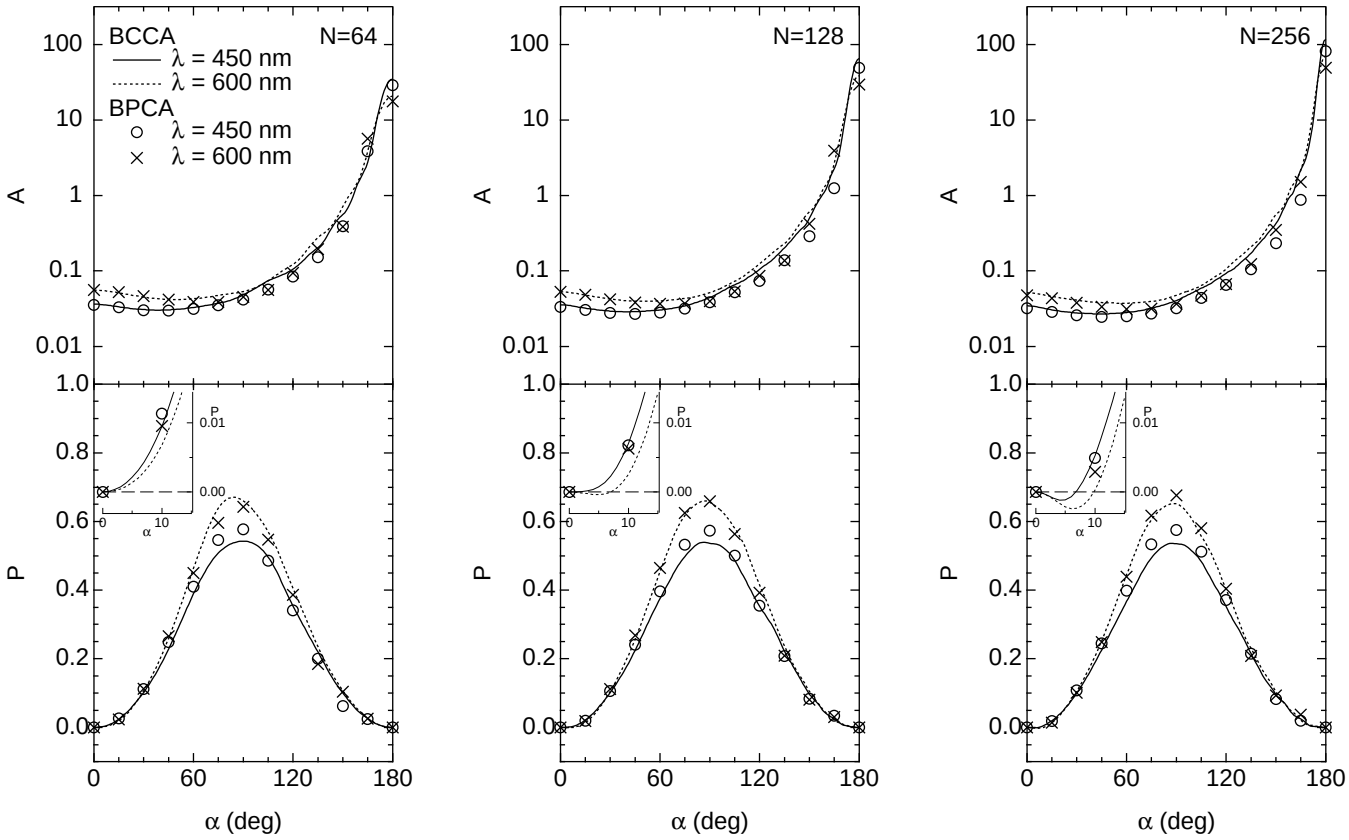

Fig. 1. Shown are the geometric albedo A and polarisation P calculated for BPCA (symbols) and BCCA (lines) particles with number of monomers $N = 64$, 128, 256 at wavelength of 450 and 600 nm. The results were obtained with the T Matrix method describing the particles as agglomerate of identical homogeneous spheres. The calculations were made for three BPCA and BCCA particles each and subsequently averaged.

Table 1
Light scattering simulations of aggregate particles and comparison to cometary dust properties.

Method	Monomer's parameters[b]				Fits[c]		Fit achieved		
used[a]	N_m	X_m	n	k	I	P	N_m	X_m	Ref.
DDA	170	0.2–0.6	1.7	0.023	−	−			[14]
DDA	8	0.6–1.8	1.7	0.023	−	+	8	1.8	[14]
DDA	256–4096	0.1	1.48	0.000029	−	−			[15]
DDA	256–4096	0.1	2.54	0.59	−	−			[15]
DDA	15	1.0–1.5	1.6–2.5	0.1–0.5	−	+[d]	15	1.0	[16]
DDA	30–200	1.2–1.9	1.29	0.008	+	+	60	1.9	[17]
DDA	30–200	1.2–1.9	1.57	0.012	+	+	200	1.2	[17]
DDA	4–10	2.6–5.2	1.65	0.01	−[e]	−[e]			[18]
DDA	4–10	2.6–5.2	1.88	0.71	−[e]	−[e]			[18]
DDA	512	0.1–0.8	1.4–1.5	0.0001–0.5	+	+[f]	512	0.68	[19]
DDA	8000	0.3	1.7	0.03	+	+	8000	0.3	[20]
TMM	1–43	0.7–2.5	1.65	0.002–0.1	−[g]	−[h]			[21]
DDA	128–8192	0.1–0.7	1.68	0.03	+	+	≥ 512	0.7	[22]
TMM	64–256	1.6	1.68	0.03	−	$\bigoplus$	> 64	1.6	[22]
DDA	128–8192	0.1–0.7	1.99	0.23	+	+	≥ 512	0.7	[22]
TMM	64–256	1.6	1.99	0.23	$\bigoplus$	−	> 64	1.6	[22]
TMM	64–256	1.0	1.98	0.48	$\bigoplus$[i]	+[i]	256	1.0	[23][j]

[a]DDA: discrete dipole approximation [12]; TMM: T-matrix method [13].
[b]N_m: the number of monomers; X_m: the size parameter of monomers; n: the real part of refractive index; k: the imaginary part of refractive index.
[c]I: intensity; P: polarisation; $\bigoplus$: a quantitative fit; +: a qualitative fit; −: no fit.
[d]For $n \geq 2.0$.
[e]A rough qualitative fit after considering a half of monomers with $m = 1.65 + 0.01\mathrm{i}$ and the other half with $m = 1.88 + 0.71\mathrm{i}$.
[f]For $k > 0.1$ as claimed after their follow-up calculations [24].
[g]A rough qualitative fit after averaging over different sizes in a power-law distribution with $X_\mathrm{m} = 1.3$ and $k = 0.01$. However, the spectral variation for the size-averaged results yields a blue colour [25].
[h]A rough quantitative fit after averaging over different sizes in a power-law distribution with $X_\mathrm{m} = 1.5$ and $k = 0.01$. The spectral variation for the size-averaged results could yield a red colour in $40 < \alpha < 100°$ [25].
[i]Not only the angular dependence but also the spectral dependence.
[j]Also in this work.

Table 2
Elemental abundances[a]

Element	Atomic weight	Carbonaceous material	Silicate (SiO_2, MgO)	Metal	Total
C	12.011	814	0	0	814
N	14.007	42	0	0	42
O	15.999	420	470	0	890
Mg	24.305	0	100	0	100
Si	28.086	0	185	0	185
Fe	55.845	0	0	52	52
Bulk density (kg m^{-3})		1.80×10^3	3.30×10^3	7.86×10^3	
Reference		[30]	[31]	[32]	

[a]The element abundances are normalized to Mg (= 100) [29].

Table 3
Refractive indices and volume fractions

Material	Wavelength		Volume	
name	450 nm	600 nm	fraction	Ref.
Amorphous carbon	$1.95 + 0.786i$	$2.14 + 0.805i$	0.4379	[35]
Organic refractory	$1.69 + 0.150i$	$1.71 + 0.149i$	0.2189	[36]
Silicate	$1.69 + 0.0299i$	$1.68 + 0.0302i$	0.3176	[37]
Metal	$2.59 + 2.77i$	$2.90 + 3.02i$	0.0256	[38]
Cometary dust[a]	$1.88 + 0.47i$	$1.98 + 0.48i$	1.0000	[23][b]

[a]Amorphous carbon is treated as the matrix.
[b]Also in this work.